Article

A Novel Six-Phase V-Shaped Flux-Switching Permanent Magnet Generator for Wind Power Generation

Pattasad Seangwong [1], Supanat Chamchuen [1], Nuwantha Fernando [2], Apirat Siritaratiwat [1] and Pirat Khunkitti [1,*]

1   Department of Electrical Engineering, Faculty of Engineering, Khon Kaen University,
    Khon Kaen 40002, Thailand
2   School of Engineering, Royal Melbourne Institute of Technology (RMIT), Melbourne, VIC 3000, Australia
*   Correspondence: piratkh@kku.ac.th; Tel.: +66-86-636-5678

Abstract: Flux-switching permanent magnet (FSPM) machines have attracted wide attention in many rotating applications that require high-power density. In this research, we propose for the first time a novel six-phase FSPM generator with a stator featuring a V-shaped flux-focusing magnet arrangement. The design is targeted for low-speed wind power generation. To achieve the design objectives as a wind generator, the highly comprehensive structural parameters, including the number of rotor poles, split ratio, and rotor pole width, are designed and optimized using 2D finite-element analysis. From findings, the optimal stator/rotor pole combination is discovered to be 12/19 for the considered power and speed requirements. When compared to the initial structure, the optimized structure of the V-shaped FSPM generator is found to produce a significant improvement in EMF, cogging torque, electromagnetic torque, power, and efficiency. The power-generating performance of the proposed FSPM generator is found to be outstanding when compared to the radial-flux PM generators described in the literature. Therefore, the proposed V-shaped FSPM generator is capable of being used for low-speed wind power generation. The machine configuration adjustment approach presented in this work can also be utilized for the design of permanent magnet wind generators.

Keywords: permanent magnet synchronous machine; permanent magnet generator; flux-switching; V-shaped; wind power generation

1. Introduction

Renewable energy has received considerable attention as an inexhaustible and nonpolluting source for power generation to lower the greenhouse effect [1–5]. Permanent magnet (PM) machines are extensively known as potential candidates for use as renewable energy power generators due to their advantages of high torque density, high efficiency, simplicity, and ease of control [6–10]. The two main types of PM machines are rotor permanent magnet machines, in which PMs are attached within the rotor part, and the stator permanent magnet (SPM) machines, which have PMs installed within the stator part. In particular, the SPM machines have attracted wide attention for renewable power generation due mainly to their lightweight rotor. The stator flux-switching permanent magnet (stator-FSPM) machines have been known as one of the efficient structures of SPM machines that are appropriate for low-speed operation [11,12]. The stator of the stator-FSPM machines is made up of laminated steel salient-pole with alternating polarities of installed PMs, while its rotor serves as a path for magnetic flux circulation to fulfill the flux-switching theory. As a result, the rotor of the stator-FSPM machines has low inertia and is simple and robust, which makes it highly suitable for low-speed wind power generation applications [10,13]. In particular, the outstanding merits of the stator-FSPM machines such as high-power density and good thermal dissipation are claimed in many literature surveys [10–14]. Nevertheless, the main drawback of the stator-FSPM machines is that their enhancement of power density may be limited when used with a large magnetic load due to its narrow armature slot area.

In particular, we noticed that the use of a V-shaped stator pole-piece with a flux-focusing magnet arrangement could effectively improve such weaknesses through an enlarged slot area. The use of V shaped poles is one of the popular techniques used for the improvement of the electromagnetic performance of FSPM machines, as shown in the following literature review. A novel 6-stator/17-rotor pole FSPM technique using magnets was proposed in 2017, showing that this structure can produce high electromagnetic torque with a low torque ripple [14]. In [15], a 6/17 FSPM machine with V-shaped teeth was proposed. It showed that this structure demonstrates low cogging torque and ripple. The authors of [16] proposed an in-wheel FSPM motor based on V-shaped magnet placement. They indicated that this structure can be a preferential candidate among different in-wheel traction motors due to the superior torque capability and efficiency. A novel sandwiched FSPM machine using V-shaped magnet placement was introduced in [17], showing that performing the V-shaped magnet placement technique can increase output torque and improve magnet usage efficiency through an enlargement of the slot area.

From the literature review on the development of FSPM machines, it is clearly seen that not only the design techniques were applied to machines for performance improvement, but it is also important to adjust and optimize the configuration of the structure since this can cause a significant improvement in the machine profiles as well. The authors in [9] showed that an adjustment of the stator configuration could yield an improvement in EMF, cogging torque, and efficiency of PM machines. It was extensively demonstrated that an improvement in EMF and output power of PM machines can be achieved by optimizing the number of poles, the split ratio, and the stator pole arc of PM machines [10,13,18–20]. In [21], it was shown that the number of stator and rotor poles of FSPM machines should be carefully optimized to achieve the higher torque capability. The authors in [22] indicated that an adjustment of stator and rotor configurations causes significant effects on EMF, cogging torque, and torque density of the FSPM machines. Since the FSPM machines have attracted research interest for use in a variety of rotating applications, including those requiring high reliability, such as aerospace power generation, large-scale wind power generation systems, automotive traction, and multiphase configurations, it has become important for such applications because it can improve the machine's fault-tolerant capability, as demonstrated in numerous previous studies [13,23–26]. It is worth noting that the multiphase configuration can also improve the torque density and provide better overload capability for FSPM machines.

According to the outstanding features of the stator-FSPM machines [10–14], it has proven to be highly capable of being used as an electrical generator for wind power generation. In particular, the V-shaped technique is an efficient approach for improving the power and torque capability of PM machines through the enhanced flux-focusing effect. Additionally, as previously mentioned, the narrow slot area is one of the main drawbacks of FSPM; implementation of the V-shaped technique could compensate for this drawback. This compensation might accordingly yield an improvement of machine efficiency through reduced copper loss. However, the use of V-shaped technique in an FSPM generator has not been reported in the literature. Therefore, as far as we know, this is the first work implementing the V-shaped technique in the FSPM generator. To provide better fault-tolerant performance and improve a higher torque density, we also propose applying the multiphase configuration to the V-shaped FSPM generator. Here, a novel six-phase V-shaped FSPM generator is proposed which was targeted for low-speed wind power generation. An optimal design of the machine's structural parameters, including the number of rotor poles, split ratio, and rotor pole width, was carried out. Designs were analyzed through simulations using the finite element method. The output characteristics of the FSPM generator, namely the flux-circulation capability, flux-linkage, EMF, cogging torque, torque, power capability, losses, and efficiency, were evaluated.

The remaining parts of this paper are arranged as follows: machine topology is shown in Section 2. Section 3 provides a description of the procedure to optimize the key

design parameters. Section 4 presents the proposed generator's performance and related discussion. Lastly, Section 5 provides a summary of this study's findings.

2. Topology of the V-shaped FSPM Generator

Figure 1a depicts the initial configuration of the proposed 6-phase V-shaped FSPM generator. It has 12 stator poles and 22 rotor poles (12-stator/22-rotor). This configuration was initialized from the 12-phase 24-slot/22-pole topology, which was claimed to be the great pole combination for FSPM wind generators [13]. The V-shaped flux-focusing magnet is designed with the goal of achieving high-power capability and efficiency of the FSPM generator. It is worth noting that an implementation of V-shaped technique theoretically yields a reduction in the initial number of phase and stator slots by a half. The topology of the V-shaped magnets was designed by setting the sandwiching pole arc to be 1.25 times the stator pole arc since this arrangement may provide great performance for the FSPM machine [17]. The concentrated armature winding is installed at the stator slots. The flux rib is designed and built for machine prototyping purposes and can be ground away following assembly. The optimal design of the 6-phase V-shaped FSPM generator with adjusted structural design parameters contains 12-stator/19-rotor poles, as depicted in Figure 1b. Both machines operate based on the principle of flux-switching, where the PMs are installed in the stator teeth with adjacent opposite polarity. The polarity of the flux-linkage is switched by a rotor rotation. The dimensions of both generators are shown in Table 1, where their design variables are defined in Figure 2.
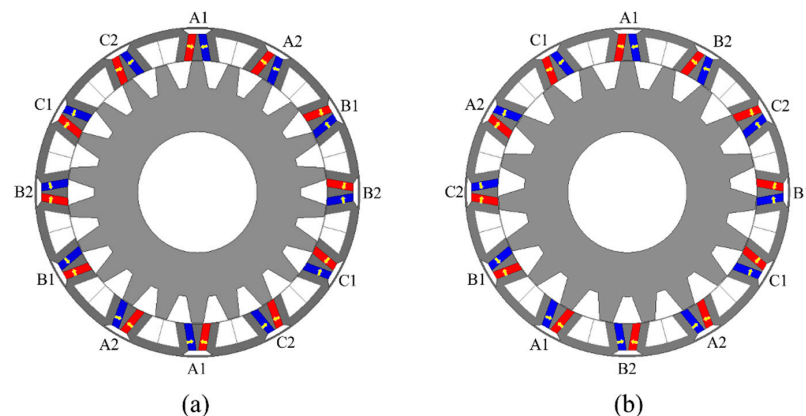

(a)   (b)

Figure 1. (**a**) The initial and (**b**) the optimal structures of 6-phase V-shaped FSPM generators.
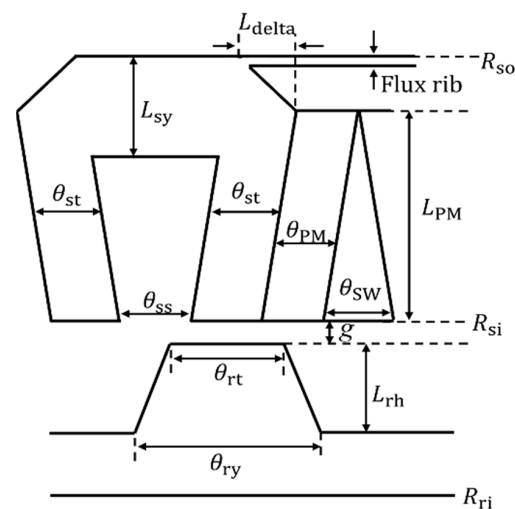

Figure 2. Design variables.

Table 1. Dimensions of the initial and the optimal V-shaped FSPM generators.

| Parameters	Unit	Initial V-Shaped Structure	Optimal V-Shaped Structure
Number of phases	phase	6	
Number of stator teeth, N_s	pole	12	
Number of rotor pole, N_r	pole	22	19
PM type	-	NdFeB	
Magnet remanence	T	1.2	
Magnet coercivity	kA/m	−909.46	
Axial length, L_s	mm	185	
Outer stator radius, R_{so}	mm	163.5	
Stator yoke length, L_{sy}	mm	8.56	
Split ratio	-	0.8	
Stator inner radius, R_{si}	mm	130.8	
Cut delta length, L_{delta}	mm	8	
Stator pole arc, θ_{st}	degree	3.9375	
Air gap length, g	mm	1	
PM arc, θ_{PM}	degree	3.375	
Rotor pole height, L_{rh}	mm	25.96	
Rotor inner radius, R_{ri}	mm	60	
Flux rib,	mm	1.5	
PM length, L_{PM}	mm	26.6	
Stator slot arc, θ_{ss}	degree	10.45	
Coil turn	turn	65	
Sandwiching pole arc, θ_{sw}	degree	4.92	
Total stator slot area	cm^2	10	
Total magnet volume	cm^3	892	
Rotor pole width ratio	-	1.4	1.6
Rotor pole arc, θ_{rt}	degree	5.25	6
Rotor pole yoke-arc, θ_{ry}	degree	12.075	13.8
Rated speed	rpm	500	

3. Optimization of Key Design Parameters

To achieve high torque and efficiency capability of the proposed V-shaped FSPM generator, we propose a design and optimize the structure to meet high suitability of a low-speed wind power generation application. In this work, the design parameters, including the number of rotor poles, split ratio, and rotor pole width, are selected since their high impact on the FSPM machines' performance has been claimed in many studies. The stepwise optimization technique was performed in the design. The sequence of the optimization parameters is prioritized based on their impact on the machine's performance. The design objective functions include the no-load EMF with its THD and cogging torque, since these parameters essentially represent the performance of the wind generator. It should be noted that the design constraints include a fixed copper loss, same PM volume with fixed V-shaped alignment, same air-gap length, and a fixed ratio of rotor pole arc and yoke arc. The selection of an optimal value for each design parameter is based on the trade-off between all objective functions whose values are suitable for wind power generation at a rated speed of 500 rpm.

3.1. Number of Rotor Poles

The number of rotor poles is typically believed to have a significant effect on the performance of PM machines since it serves as a major flux path and is used for alternating the magnetic field circulation of the FSPM machines. The formula describing the possible number of stator pole N_s and rotor pole N_r combinations for the FSPM machine is given by Equation (1);

$$\frac{N_s}{HCD(N_s, N_r)} = 6i \tag{1}$$

where *HCD* is the highest common divisor and *i* is an integer [11]. Figure 3 depicts the effects of the variation in the number of rotor poles on the machine's EMF, THD, and cogging torque. It demonstrates that changing the number of rotor poles can rapidly increase the EMF magnitude, even significantly higher than that of the initial structure. The greatly improved EMF is caused by highly improved magnetic field utilization due to better distribution of the magnetic field circulation. Additionally, the THD is slightly affected by the rotor pole variation. Figure 3b shows that the cogging torque rapidly increases at some rotor pole numbers, while it can be greatly reduced at the rotor pole number of 17, 19, and 23. It is seen that changes in rotor pole numbers have a significant effect on the cogging torque scale since the rotor tooth is typically used as a magnetic flux-circulation path. As a result, the rotor pole number that provides a more balanced magnetic field distribution typically yields lower cogging torque. Results clearly show that the V-shaped FSPM generator with 19 rotor teeth outperforms other structures since it can produce a very high EMF with the lowest cogging torque while maintaining the THD scale. Therefore, the V-shaped FSPM generator with 12-stator/19-rotor is selected for further performance improvement. The EMF phasors of the initial 12-stator/22-rotor and the 12-stator/19-rotor structure are demonstrated in Figure 4, showing that each phase winding is constituted by connecting two coils to achieve symmetrical phase EMF waveforms.

(a)   (b)
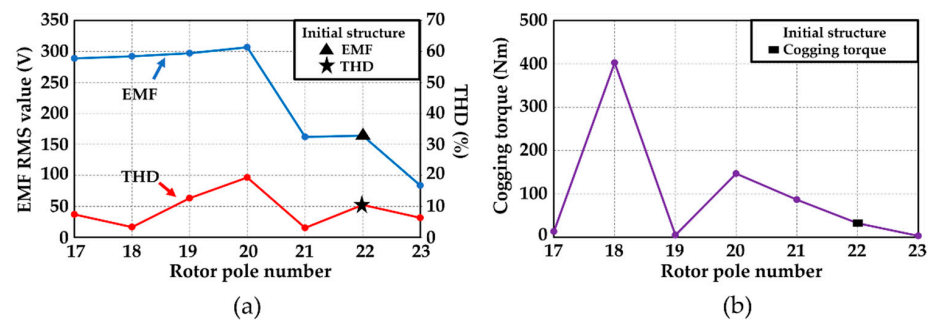
Figure 3. Influence of rotor pole number on the (**a**) EMF profile and (**b**) cogging torque of the V-shaped FSPM generators with a 12-slot stator.


(a)   (b)
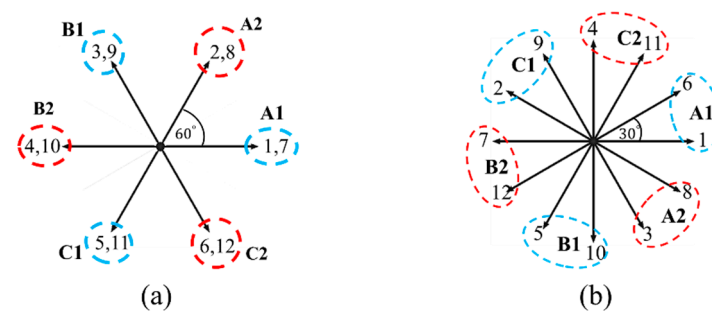
Figure 4. Phase EMF phasors of the 6-phase V-shaped FSPM generators: (**a**) initial 12-stator/22-rotor structure; (**b**) 12-stator/19-rotor structure.

3.2. Split Ratio

The split ratio of FSPM machines is generally defined as R_{si}/R_{so}. This parameter typically plays an important role in the machine's performance since it is highly related to many parts of the machine's configuration. Here, we evaluated the machine's no-load capability by varying the split ratio from 0.6 to 0.9. It is noted that the split ratio of the initial structure is 0.8. Figure 5 depicts the EMF, THD, and cogging torque of the 12-stator/19-rotor V-shaped FSPM generator with various split ratios. It demonstrates that changing the split ratio, apart from the conventional value of 0.8, results in a reduction in EMF. A reduction in EMF at lower split ratios is caused primarily by flux-leakage between the stator teeth and the rotor shaft, whereas reduced magnetic saturation capability is the main cause of

lower EMF at higher split ratios. These reduced flux utilization capabilities also yield an increased THD, along with a lower cogging torque resulting from a decrease in energy in the air gap. To maintain an acceptable THD value, the split ratio should be kept between 0.7 and 0.8. The trade-off reveals that the optimal split ratio should be 0.8, owing to its highest EMF, acceptable THD, and moderate cogging torque.
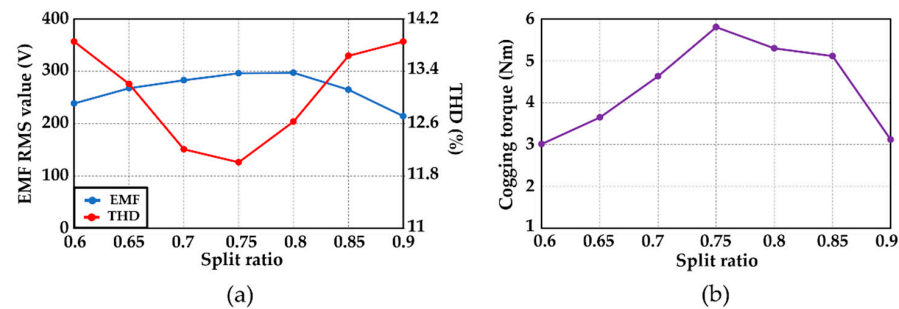
Figure 5. Influence of the split ratio on the (**a**) EMF profile and (**b**) cogging torque of the 12-stator/19-rotor V-shaped FSPM generators.

3.3. Rotor Pole Width

The width of rotor teeth typically indicates a huge impact on the shape of the magnetic flux path, mainly at the air gap. Therefore, it has a major impact on the machine's performance, especially the cogging torque scale. Here, we propose varying the rotor pole width of the 12-stator/19-rotor V-shaped FSPM generator having the optimal split ratio of 0.8, aiming to improve machine capability for wind power generation. The rotor pole width ratio was varied from 1 to 1.9, where the initial rotor pole width of one-quarter times the stator pole pitch was defined as a rotor pole width ratio equal to 1. Figure 6 depicts the effect of rotor pole width variation on the machine's EMF, THD, and cogging torque. It shows that the EMF of the V-shaped FSPM generator improves by increasing the rotor pole width ratio from the conventional value of 1.4 to 1.5; thereafter, it decreases continuously. Meanwhile, decreasing the rotor pole width below 1.4 causes a rapid reduction in EMF. Higher EMF scales are obtained due to the better compatibility of the width of rotor teeth with respect to the shape of the stator teeth; as a result, the magnetic flux can be greatly linked between the stator and rotor, resulting in better flux utilization. In addition, we found that the THD scale is inversely proportional to the rotor pole width. The cogging torque profile shows that the rotor pole width has a huge impact on the cogging torque amplitude since the width of rotor tooth is typically associated with an interacting force between the stator and rotor teeth in the initial situation. Our analysis revealed that the structures with an appropriate rotor pole width demonstrate a low cogging torque scale due to the lower flux-leakage at the rotor tooth and stator tooth. The trade-off indicates that the optimal rotor pole width is selected as 1.6 because of its high EMF, low THD, and significantly improved cogging torque.
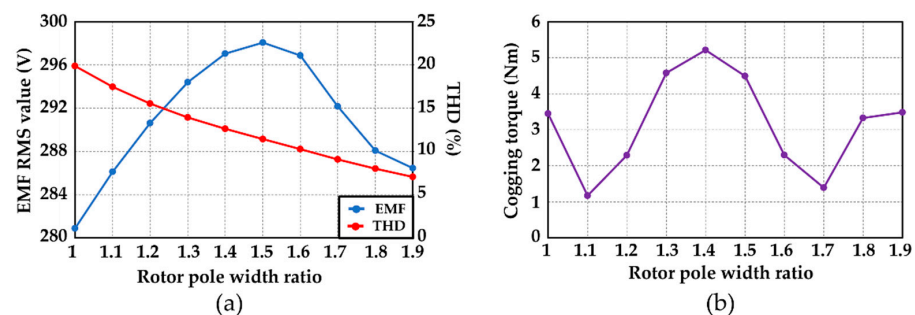

Figure 6. Influence of the rotor pole width on the (**a**) EMF profile and (**b**) cogging torque of the 12-stator/19-rotor V-shaped FSPM generators.

4. Comparison of Generator Performance

From the previous section, we found that the optimal design of the 6-phase V-shaped FSPM generator is a structure having 12-stator/19-rotor poles, a split ratio of 0.8, and a rotor pole width ratio of 1.6. In this section, the electromagnetic performance of the optimal structure is evaluated and compared to that of the initial configuration. The no-load performance indicators include the flux-circulation capability, flux-linkage, EMF, and cogging torque, while the on-load characteristics are the electromagnetic torque, power capability, losses, and efficiency. To provide a fair comparison, two FSPM generators are compared under the identical copper loss condition at 500 rpm rated speed.

### 4.1. PM Flux-Line Distribution

Figure 7 illustrates a comparison of the PM flux-line distributions of the initial and optimal design of V-shaped FSPM generators. It is apparent that the optimized structure demonstrates considerably lower leakage flux than the initial one, especially between the teeth. Additionally, the better flux-focusing capability of the optimal structure is observed, especially at the rotor. In addition, the optimal structure has greater magnetic saturation, especially at the stator. This improved property implies better magnet utilization of the optimal structure, which might contribute to the improvement in performance.
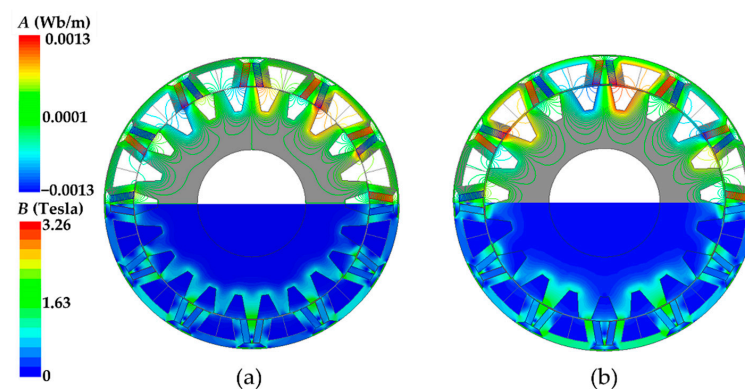
Figure 7. PM flux-line distributions: (**a**) initial V-shaped structure; (**b**) optimal V-shaped structure.

4.2. Flux-Linkage and EMF

The flux-linkage and EMF profiles of the initial and optimal V-shaped FSPM generators during the open-circuit condition are illustrated in Figures 8 and 9, respectively. It is seen that the optimized V-shaped FSPM generator produces significantly higher flux-linkage and EMF than the initial structure, due mainly to its better flux-focusing capability. The EMF produced by the optimized structure is almost twice as high as that of the initial one. However, the slightly higher THD of the optimized structure (10.3%) than the initial value (8.4%) is indicated due to the odd number of rotor poles. The huge improvement in the EMF scale could possibly yield a significant enhancement in power generation capability.
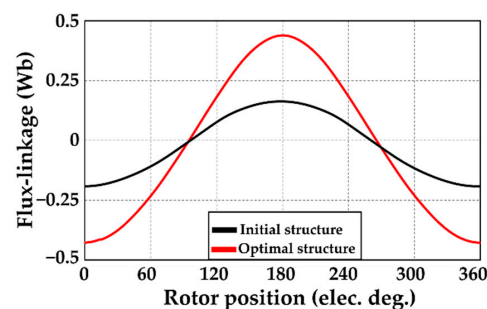
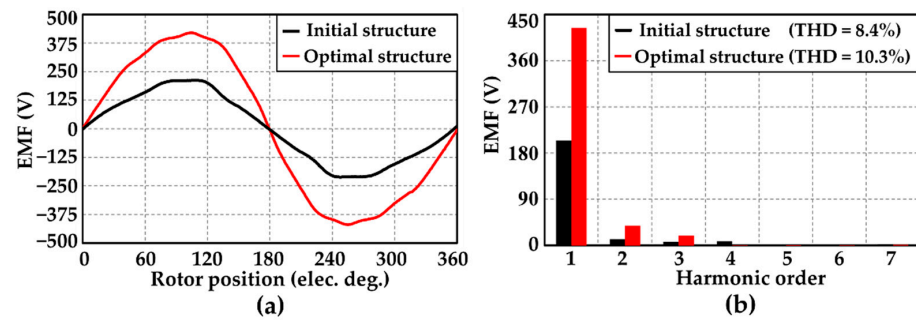**Figure 8.** Comparison of flux-linkage.

Figure 9. Comparison of (**a**) back-EMF waveforms and (**b**) contributing spectrum.

4.3. Cogging Torque

The cogging torque is typically an important parameter related to the starting performance of PM machines, especially for low-speed wind power generation. According to Figure 10, it shows that the optimal V-shaped FSPM generator has approximately 14.3 times lower cogging torque than the initial design, thus demonstrating its outstanding suitability for low-speed operation.
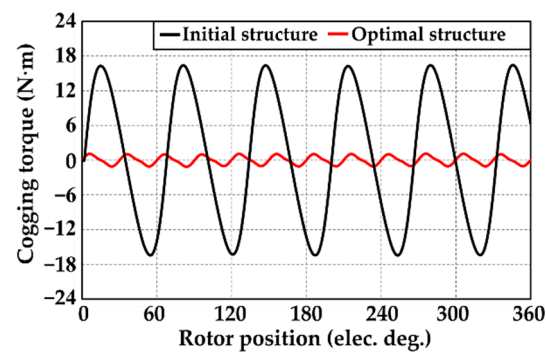

Figure 10. Comparison of cogging torque.

4.4. On-Load-Generating Performance

On-load torque characteristics of two V-shaped FSPM generators are shown in Figure 11. It reveals that the optimized structure can produce 2.7 times higher torque with significantly lower torque ripple (T_{ripple}) than the initial structure, which clearly indicates the better torque capability of the optimized structure. Table 2 presents a comparison of the overall performance of the V-shaped FSPM generators at their rated speed of 500 rpm. It is seen that the output voltage of the optimized structure is 1.7 times higher than that produced by the initial one. Remarkably, the output power of the optimized V-shaped FSPM generator is 73.6% improved from the initial configuration, which reaches 15.6 kW. A slightly higher level of core losses is observed mainly due to the comparatively high flux densities and high level of saturation, while the unbalanced flux circulation from an odd number of rotor poles causes slight enhancement of eddy current losses. Overall, the efficiency of the optimized structure is 1.79% higher than that of the initial structure, which reaches 93.28%. For future work, it is recommended to include the experimental verification.

4.5. Comparison of Power-Generating Performance to the Existing Radial-Flux PM Generators

The power-generating performance of the proposed 6-phase 12-stator/19-rotor V-shaped FSPM generator is compared to the other existing radial-flux PM generators, as shown in Table 3. It reveals that the proposed V-shaped FSPM generator can produce a high power density of up to 1004.3 kW/m^3, which is very high compared to the existing radial-flux PM generators. Therefore, it clearly indicates that the proposed optimized 6-phase 12-stator/19-rotor V-shaped FSPM generator is a structure with superior characteristics beneficial for use in low-speed wind power generation.
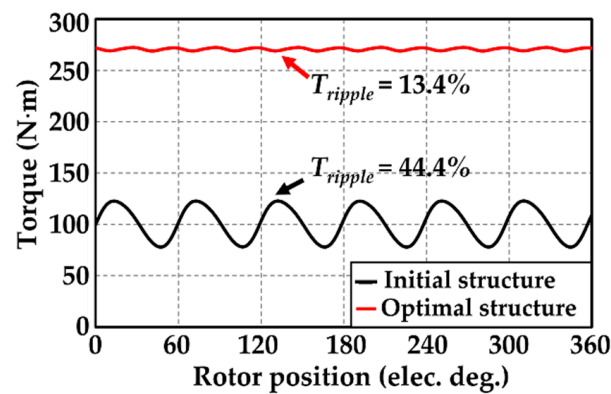
Figure 11. Comparison of electromagnetic torque waveform.

Table 2. Performance comparisons at the rated speed of 500 rpm.

Output Parameters (Unit)	Initial V-Shaped Structure	Optimal V-Shaped Structure
Open-circuit phase EMF (V_{rms})	155.3	296.9
THD (%)	8.4	10.3
Output voltage (V_{rms})	149.8	260.1
Peak–peak cogging torque (N·m)	32.9	2.3
Phase current (A)	10	
Output power (W)	8988	15,603.9
Output torque (N·m)	101.3	271
Power density (kW/m^3)	578.5	1004.3
Torque density (kN·m/m^3)	6.5	17.4
Torque ripple (%)	44.4	13.4
Copper loss (W)	326.54	
Core loss (W)	226.4	366.7
PM eddy current loss (W)	253.1	284.7
Efficiency (%)	91.49	93.28

Table 3. A comparison of power density with other radial-flux PM generators.

Reference	Power Density (kW/m^3)
Proposed structure	1004.3
[13]	1203.6
[27]	1162.5
[28]	1004.1
[29]	939.7
[30]	768.2
[31]	692.6
[32]	681.7
[33]	636.2
[34]	606.1
[35]	499.4
[36]	432.9
[37]	417.2
[38]	217.9

5. Conclusions

In this paper, a V-shaped flux-focusing magnet arrangement is applied in the design of an FSPM generator for the first time. A novel 6-phase V-shaped FSPM generator was introduced, which was designed for low-speed wind power generation. The structural parameters of the proposed generator, including the number of rotor poles, split ratio, and

rotor pole width were designed and optimized to achieve enhanced power production and high efficiency together with low cogging torque. It was found that the 12-stator/19-rotor was an optimal combination of stator/rotor poles for this structure. After optimizing the design parameters of the 6-phase 12/19 poles V-shaped FSPM generator, it was discovered that the optimal structure produced 91.18% increased EMF, 14.3 times lower cogging torque, 73.6% improved electromagnetic torque and power, and 1.79% higher efficiency, compared to the initial structure. The generator can produce output power of up to 15.6 kW at rated conditions, which is very high when compared to existing radial-flux PM generators. Therefore, the proposed 6-phase 12-stator/19-rotor V-shaped FSPM generator becomes another capable choice for low-speed wind power generation. The machine configuration adjustment approach presented in this paper can be utilized for the design of permanent magnet generators.

Author Contributions: Conceptualization, P.S. and P.K.; methodology, P.S.; software, P.S.; data curation, P.S.; formal analysis, P.S.; writing—original draft, P.S.; visualization, S.C., N.F., and A.S.; validation, P.K.; supervision, P.K.; funding acquisition, P.K.; writing—review and editing, P.K. All authors have read and agreed to the published version of the manuscript.

Data Availability Statement: Not applicable.

References

1. Huang, C.; Li, F.; Jin, Z. Maximum Power Point Tracking Strategy for Large-Scale Wind Generation Systems Considering Wind Turbine Dynamics. *IEEE Trans. Ind. Electron.* **2015**, *62*, 2530–2539. [CrossRef]
2. Polinder, H.; Ferreira, J.A.; Jensen, B.B.; Abrahamsen, A.B.; Atallah, K.; McMahon, R.A. Trends in Wind Turbine Generator Systems. *IEEE J. Emerg. Sel. Topics Power Electron.* **2013**, *1*, 174–185. [CrossRef]
3. Boonluk, P.; Khunkitti, S.; Fuangfoo, P.; Siritaratiwat, A. Optimal Siting and Sizing of Battery Energy Storage: Case Study Seventh Feeder at Nakhon Phanom Substation in Thailand. *Energies* **2021**, *14*, 1458. [CrossRef]
4. Srithapon, C.; Ghosh, P.; Siritaratiwat, A.; Chatthaworn, R. Optimization of Electric Vehicle Charging Scheduling in Urban Village Networks Considering Energy Arbitrage and Distribution Cost. *Energies* **2020**, *13*, 349. [CrossRef]
5. Boonluk, P.; Siritaratiwat, A.; Fuangfoo, P.; Khunkitti, S. Optimal Siting and Sizing of Battery Energy Storage Systems for Distribution Network of Distribution System Operators. *Batteries* **2020**, *6*, 56. [CrossRef]
6. Chen, H.; El-Refaie, A.M.; Demerdash, N.A.O. Flux-Switching Permanent Magnet Machines: A Review of Opportunities and Challenges—Part I: Fundamentals and Topologies. *IEEE Trans. Energy Convers.* **2020**, *35*, 684–698. [CrossRef]
7. Nobahari, A.; Aliahmadi, M.; Faiz, J. Performance Modifications and Design Aspects of Rotating Flux Switching Permanent Magnet Machines: A Review. *IET Electr. Power Appl.* **2020**, *14*, 1–15. [CrossRef]
8. Nissayan, C.; Seangwong, P.; Chamchuen, S.; Fernando, N.; Siritaratiwat, A.; Khunkitti, P. Modeling and Optimal Configuration Design of Flux-Barrier for Torque Improvement of Rotor Flux Switching Permanent Magnet Machine. *Energies* **2022**, *15*, 8429. [CrossRef]
9. Lounthavong, V.; Sriwannarat, W.; Siritaratiwat, A.; Khunkitti, P. Optimal Stator Design of Doubly Salient Permanent Magnet Generator for Enhancing the Electromagnetic Performance. *Energies* **2019**, *12*, 3201. [CrossRef]
10. Sriwannarat, W.; Seangwong, P.; Lounthavong, V.; Khunkitti, S.; Siritaratiwat, A.; Khunkitti, P. An Improvement of Output Power in Doubly Salient Permanent Magnet Generator Using Pole Configuration Adjustment. *Energies* **2020**, *13*, 4588. [CrossRef]
11. Zhu, Z.Q.; Chen, J.T. Advanced Flux-Switching Permanent Magnet Brushless Machines. *IEEE Trans. Magn.* **2010**, *46*, 1447–1453. [CrossRef]
12. Cheng, M.; Hua, W.; Zhang, J.; Zhao, W. Overview of Stator-Permanent Magnet Brushless Machines. *IEEE Trans. Ind. Electron.* **2011**, *58*, 5087–5101. [CrossRef]
13. Shao, L.; Hua, W.; Soulard, J.; Zhu, Z.Q.; Wu, Z.; Cheng, M. Electromagnetic Performance Comparison between 12-Phase Switched Flux and Surface-Mounted Pm Machines for Direct-Drive Wind Power Generation. *IEEE Trans. Ind. Appl.* **2020**, *56*, 1408–1422. [CrossRef]
14. Zhao, G.; Hua, W. A Novel Flux-Switching Permanent Magnet Machine with v-Shaped Magnets. *AIP Adv.* **2017**, *7*, 056655. [CrossRef]
15. Zhao, G.; Hua, W. Comparative Study between a Novel Multi-Tooth and a V-Shaped Flux-Switching Permanent Magnet Machines. *IEEE Trans. Magn.* **2019**, *55*, 1–8. [CrossRef]
16. Zhu, X.; Shu, Z.; Quan, L.; Xiang, Z.; Pan, X. Design and Multicondition Comparison of Two Outer-Rotor Flux-Switching Permanent-Magnet Motors for in-Wheel Traction Applications. *IEEE Trans. Ind. Electron.* **2017**, *64*, 6137–6148. [CrossRef]

17. Zhou, Y.J.; Zhu, Z.Q. Torque Density and Magnet Usage Efficiency Enhancement of Sandwiched Switched Flux Permanent Magnet Machines Using V-Shaped Magnets. *IEEE Trans. Magn.* **2013**, *49*, 3834–3837. [CrossRef]

18. Sriwannarat, W.; Siritaratiwat, A.; Khunkitti, P. Structural Design of Partitioned Stator Doubly Salient Permanent Magnet Generator for Power Output Improvement. *Adv. Mater. Sci. Eng.* **2019**, *2019*, 2189761. [CrossRef]

19. Sriwannarat, W.; Khunkitti, P.; Janon, A.; Siritaratiwat, A. An Improvement of Magnetic Flux Linkage in Electrical Generator Using the Novel Permanent Magnet Arrangement. *Acta Phys. Pol. A* **2018**, *133*, 642–644. [CrossRef]

20. Sriwannarat, W.; Seangwong, P.; Siritaratiwat, A.; Fernando, N.; Dechgummarn, Y.; Khunkitti, P. Electromagnetic Torque Improvement of Doubly Salient Permanent Magnet Machine Using Pole Ratio Adjustment Technique. *Front. Energy Res.* **2021**, *9*, 1–10. [CrossRef]

21. Hua, W.; Zhang, G.; Cheng, M. Investigation and Design of a High-Power Flux-Switching Permanent Magnet Machine for Hybrid Electric Vehicles. *IEEE Trans. Magn.* **2015**, *51*, 1–5. [CrossRef]

22. Zhu, X.; Shu, Z.; Quan, L.; Xiang, Z.; Pan, X. Multi-Objective Optimization of an Outer-Rotor V-Shaped Permanent Magnet Flux Switching Motor Based on Multi-Level Design Method. *IEEE Trans. Magn.* **2016**, *52*, 1–8. [CrossRef]

23. Yu, F.; Cheng, M.; Chau, K.T. Controllability and Performance of a Nine-Phase FSPM Motor under Severe Five Open-Phase Fault Conditions. *IEEE Trans. Energy Convers.* **2016**, *31*, 323–332. [CrossRef]

24. Xue, X.; Zhao, W.; Zhu, J.; Liu, G.; Zhu, X.; Cheng, M. Design of Five-Phase Modular Flux-Switching Permanent-Magnet Machines for High Reliability Applications. *IEEE Trans. Magn.* **2013**, *49*, 3941–3944. [CrossRef]

25. Thomas, A.S.; Zhu, Z.Q.; Owen, R.L.; Jewell, G.W.; Howe, D. Multiphase Flux-Switching Permanent-Magnet Brushless Machine for Aerospace Application. *IEEE Trans. Ind. Appl.* **2009**, *45*, 1971–1981. [CrossRef]

26. Taha, M.; Wale, J.; Greenwood, D. Greenwood Design of a High Power-Low Voltage Multiphase Permanent Magnet Flux Switching Machine For Automotive Applications. In Proceedings of the 2017 IEEE International Electric Machines & Drives Conference (IEMDC), Miami, FL, USA, 21–24 May 2017.

27. Li, F.; Zhu, X. Comparative Study of Stepwise Optimization and Global Optimization on a Nine-Phase Flux-Switching Pm Generator. *Energies* **2021**, *14*, 4754. [CrossRef]

28. Shao, L.; Hua, W.; Zhu, Z.Q.; Tong, M.; Zhao, G.; Yin, F.; Wu, Z.; Cheng, M. Influence of Rotor-Pole Number on Electromagnetic Performance in 12-Phase Redundant Switched Flux Permanent Magnet Machines for Wind Power Generation. *IEEE Trans. Ind. Appl.* **2017**, *53*, 3305–3316. [CrossRef]

29. Shao, L.; Hua, W.; Li, F.; Soulard, J.; Zhu, Z.Q.; Wu, Z.; Cheng, M. A Comparative Study on Nine- and Twelve-Phase Flux-Switching Permanent-Magnet Wind Power Generators. *Proc. Conf. IEEE Trans. Ind. Appl.* **2019**, *55*, 3607–3616. [CrossRef]

30. Li, F.; Hua, W.; Tong, M.; Zhao, G.; Cheng, M. Nine-Phase Flux-Switching Permanent Magnet Brushless Machine for Low-Speed and High-Torque Applications. *IEEE Trans. Magn.* **2015**, *51*, 8700204.

31. Tlali, P.M.; Wang, R.J.; Gerber, S.; Botha, C.D.; Kamper, M.J. Design and Performance Comparison of Vernier and Conventional PM Synchronous Wind Generators. *IEEE Trans. Ind. Appl.* **2020**, *56*, 2570–2579. [CrossRef]

32. Kim, B. Design Method of a Direct-Drive Permanent Magnet Vernier Generator for a Wind Turbine System. *Proc. Conf. IEEE Trans. Ind. Appl.* **2019**, *55*, 4665–4675. [CrossRef]

33. Labuschagne, C.J.J.; Kamper, M.J. Design and Performance Evaluation of PM Vernier Generator Technology for a Small-Scale Uncontrolled Passive Wind Generator System. *IEEE Trans. Ind. Appl.* **2022**, *58*, 4657–4667. [CrossRef]

34. Ullah, W.; Khan, F.; Hussain, S. A Novel Dual Rotor Permanent Magnet Flux Switching Generator for Counter Rotating Wind Turbine Applications. *IEEE Access.* **2022**, *10*, 16456–16467. [CrossRef]

35. Zhao, X.; Niu, S.; Fu, W. Sensitivity Analysis and Design Optimization of a New Hybrid-Excited Dual-PM Generator with Relieving-DC-Saturation Structure for Stand-Alone Wind Power Generation. *IEEE Trans. Magn.* **2020**, *56*, 1–5. [CrossRef]

36. Nasiri-Zarandi, R.; Ajamloo, A.M.; Abbaszadeh, K. Design Optimization of a Transverse Flux Halbach-Array PM Generator for Direct Drive Wind Turbines. *IEEE Trans. Energy Convers.* **2020**, *35*, 1485–1493. [CrossRef]

37. Geng, H.; Zhang, X.; Tong, L.; Qingzhi, M.; Mingjun, X.; Zhang, Y.; Wang, L. Performance Optimization Analysis of Hybrid Excitation Generator with the Electromagnetic Rotor and Embedded Permanent Magnet Rotor for Vehicle. *IEEE Access.* **2021**, *9*, 163640–163653. [CrossRef]

38. Seangwong, P.; Siritaratiwat, A.; Sriwannarat, W.; Fernando, N.; Khunkitti, P. Design of Doubly Salient Permanent Magnet Generator for Output Power Enhancement Using Structural Modification. *J. Appl. Comput. Mech.* **2021**, *7*, 2171–2178.